TOWARDS REAL-TIME FRACTIONATION OF MIXED-PHASE PRECIPITATION

Eric R. Pardyjak[1]*, Dhiraj K. Singh[1], Daniel Webster[1], Benjamin H. Silberman[1], Timothy Garrett[2], and Travis Morrison[1,3]

1 University of Utah, Department of Mechanical Engineering, Salt Lake City, UT, USA
2 University of Utah, Department of Atmospheric Sciences, Salt Lake City, UT, USA
3 Utah Avalanche Center, Salt Lake City, UT, USA
** Indicates the presenting author*

ABSTRACT: Near-surface precipitation can occur as liquid, solid, or mixed-phase hydrometeors. In many winter storms, individual particles are not purely rain or snow, but instead contain both liquid and ice, as in sleet, freezing rain, or partially melted snow. These complex particles remain poorly constrained in observations, which limits progress in numerical weather prediction and in understanding hazardous winter weather. Mixed-phase precipitation is especially important because it strongly affects surface icing, visibility, and road traction, creating major risks for transportation and infrastructure. From a snowpack perspective, the water content of precipitation can lead to the injection of both heat and liquid mass into the snowpack resulting in snow grain metamorphism and potentially modification of the seasonal release of snow-melt water, flooding, weakening of a snowpack, and generation of various melt-freeze crusts that lead to avalanche instabilities. Various methods currently exist for quantifying the amount of water going into a snowpack including optical disdrometers, imaging disdrometers, micro rain radars, and integrated satellite products, each of which has advantages and disadvantages. Crowdsourcing has also provided important qualitative knowledge of the spatial variability of phase that is particularly useful for validation studies. Here, we present a new first-principles-based experimental methodology based on the Differential Emissivity Imaging Disdrometer or DEID, a thermal-imaging hot-plate device, that has previously been used to measure snow water equivalent (SWE), snow density, and other integrated snowpack properties. Because the DEID can analyze hydrometeors on a particle-by-particle basis, it can be used to identify very short-lived mixed-phase events that may normally be overlooked. We present cold-room lab results to verify that the methodology works and to quantify its ability to fractionate liquid and ice phases. We then present preliminary results of phase-fractionation from field observations collected in Utah at the Alta-Collins snow-study plot and Red Butte Canyon during the 2020–2021 winter season and more recently at the Atwater snow-study plot during the 2025-2026 winter season. We analyze storms with a range of near-freezing mean air temperatures representing different conditions.

KEYWORDS: Mixed-phase precipitation, DEID, Avalanche forecasting, Rain-on-snow events.

1. INTRODUCTION

The phase of precipitation strongly influences hydrologic, atmospheric, and cryospheric processes. Whether precipitation reaches the surface as rain, snow, or a combination of both determines the transfer of mass and energy to the surface and directly affects snowpack evolution, streamflow, infrastructure icing, transportation safety, and numerical weather prediction. During winter storms, precipitation frequently transitions between liquid and solid phases as atmospheric temperature, humidity, and vertical thermodynamic structure evolve. These transitions often occur over relatively short temporal and spatial scales, making them particularly difficult to observe and quantify. Although precipitation is commonly classified as either rain or snow, many winter storms contain mixed-phase hydrometeors in which individual particles consist of both liquid water and ice, including sleet, freezing rain, partially melted snowflakes, and wet snow. Quantifying the liquid and frozen fractions within individual hydrometeors remains an important observational challenge in winter precipitation research.

Accurate measurements of precipitation phase are particularly important in mountainous regions, where small variations in temperature can produce rapid transitions between rain, snow, and mixed-phase precipitation. These transitions strongly influence snowpack accumulation, snow density, snow water equivalent (SWE), and the formation of melt-freeze crusts. Liquid water entering an existing snowpack not only adds mass but also transfers sensible and latent heat, accelerating snow metamorphism and altering the mechanical properties of the snowpack. Such changes influence snow stability and can contribute to wet-snow and rain-on-snow avalanche

* Corresponding author address:
Eric R. Pardyjak, University of Utah,1495 E 100 S,
Salt Lake City, UT 84112; tel: +1 802 585 5588
email: eric.pardyjak@utah.ed

conditions. Accurate knowledge of precipitation phase is also essential for improving hydrologic forecasting, understanding flood generation during rain-on-snow events, and validating numerical weather prediction models under near-freezing atmospheric conditions.

Many instruments and observational approaches have been developed to estimate precipitation phase and precipitation properties. Optical disdrometers measure particle size and fall velocity to infer precipitation type through empirical relationships between particle diameter, fall speed, and hydrometeor class (Fehlmann et al., 2020). Imaging disdrometers (Grazioli et al., 2014) extend these capabilities by capturing particle images that enable classification based on particle morphology and shape. Micro Rain Radars (MRRs) provide vertical profiles of radar reflectivity and Doppler velocity, allowing precipitation structure to be inferred throughout the atmospheric column and helping identify melting layers and transitions between rain and snow (García-Benadí et al., 2020). Satellite observations provide broad spatial coverage by combining visible, infrared, and microwave measurements to estimate precipitation phase over regional and global scales (Prigent, 2010; Zhao et al., 2024). In recent years, crowdsourced weather observations have also become valuable for identifying spatial variations in precipitation phase, particularly during high-impact winter storms, and have provided useful datasets for model evaluation and validation (Jennings et al., 2023).

Despite these advances, existing observational techniques primarily classify precipitation as rain, snow, or mixed precipitation at the bulk scale and generally do not directly quantify the liquid and frozen mass fractions within individual hydrometeors. Optical and imaging disdrometers rely primarily on particle geometry, fall velocity, or image appearance, which can become ambiguous for partially melted or irregular particles. Radar and satellite observations provide valuable large-scale information but lack the spatial resolution needed to resolve individual hydrometeors near the surface, while crowdsourced observations provide useful qualitative information but cannot directly measure particle composition. This observational gap is particularly important near 0 °C, where rapid phase transitions can affect surface icing and transportation hazards and alter the transfer of liquid water and heat into the snowpack. For snow-covered terrain, these processes can influence snow metamorphism, melt-freeze crust formation, snowpack stability, and rain-on-snow runoff. Therefore, a measurement approach capable of directly and independently quantifying the frozen and liquid components of individual hydrometeors is needed.

In this study, we present a new first-principles methodology for particle-by-particle phase fractionation using the Differential Emissivity Imaging Disdrometer (DEID), a thermal-imaging hot-plate instrument previously developed for measuring particle mass, snow water equivalent, snowfall density, and other precipitation properties (Singh et al., 2021; Morrison et al., 2023; Singh et al., 2024). Rather than relying on particle shape, fall velocity, or other empirical classification methods (Jia et al., 2019; Locatelli et al., 1974), the proposed methodology analyzes the thermal evolution of individual hydrometeors during melting and evaporation to independently estimate frozen and liquid water mass using energy conservation. Comparison of these independently estimated masses enables direct determination of the frozen and liquid fractions within each hydrometeor, allowing precipitation to be classified as pure snow, pure rain, or mixed-phase precipitation.

Laboratory experiments are first used to validate the methodology under controlled conditions, followed by preliminary demonstrations using field observations collected during winter storms in northern Utah. The proposed methodology introduces a new capability that is still under development that aims to yield real-time, particle-by-particle characterization of mixed-phase precipitation and provides a foundation for improved observations of winter precipitation, rain-on-snow events, and snowpack processes.

2. THE DEID TECHNOLOGY

The DEID is a thermal-imaging hot-plate instrument developed for particle-by-particle characterization of hydrometeors (Singh et al., 2021; Morrison et al., 2023; Singh et al., 2024). The system consists of a low-emissivity aluminum plate maintained at a prescribed temperature and viewed by a calibrated infrared camera (Fig. 1). Because the aluminum surface has a very low emissivity (≈0.1), its apparent radiative temperature is significantly lower than that of incoming hydrometeors, producing strong radiative temperature contrast and enabling detection and tracking of individual particles.

Unlike conventional precipitation sensors, the DEID applies a first-principles energy balance to each individual hydrometeor. The control volume is defined as the particle itself rather than the entire heated plate. Consequently, only the heat transferred from the heated surface to the particle is considered in the energy balance, while heat exchange occurring elsewhere on the plate does not contribute to the particle mass estimation. This particle-based control volume makes the measurement largely independent of ambient environmental conditions, including wind speed, air

temperature, and relative humidity, provided that the plate temperature remains well controlled.

Previous studies have demonstrated that DEID can directly measure particle mass, effective size, snowfall density, snow water equivalent (SWE), and other microphysical properties on a particle-by-particle basis using first-principles heat-transfer analysis (Singh et al., 2021; Morrison et al., 2023; Singh et al., 2024). In the present study, the existing DEID framework is extended to estimate the liquid and frozen fractions of individual hydrometeors during mixed-phase precipitation events. The DEID melting method estimates the mass of the frozen component by applying the energy balance during the melting period, whereas the DEID evaporation method estimates hydrometeor mass from the subsequent evaporation process. The masses estimated using the two methods are expressed as follows:

Melting method:

$$m_{\mathrm{ice}} = \frac{\tilde{k}}{C_{\mathrm{ice}}(0° - T_{0,\mathrm{ice}}) + L_f} \int_0^{\Delta t_{\mathrm{melt}}} A_{\mathrm{ice}}(t)\left(T_p - T_{\mathrm{ice}}(t)\right) dt,$$

Evaporation method:

$$m_{\mathrm{liq}} = \frac{\tilde{k}}{C_{\mathrm{liq}}(T_p - 0°) + L_v} \int_0^{\Delta t_{\mathrm{evap}}} A_{\mathrm{liq}}(t)\left(T_p - T_{\mathrm{liq}}(t)\right) dt,$$

where $\tilde{k}$ is a calibration constant; C_{ice} and C_{liq} are the specific heats of ice and liquid water, respectively; T_p is the hotplate temperature; $T_{0,ice}$ is the initial temperature of the frozen hydrometeor when it reaches the plate; $T_{ice}(t)$ and $T_{liq}(t)$ are the temperatures of the frozen and liquid components at time *t*, respectively; $A_{ice}(t)$ and $A_{liq}(t)$ are the corresponding particle areas during melting and evaporation; L_f and L_v are the latent heats of fusion and vaporization of water, respectively; and Δt_{melt} and Δt_{evap} are the melting and evaporation times. The standard DEID field configuration uses a low-emissivity aluminum plate maintained at approximately 85 °C. During previous field deployments, this configuration generally produced an apparent radiative background temperature of approximately 5-10°C, providing strong thermal contrast for detecting frozen hydrometeors with a thermal camera. However, a plate temperature of 85 °C is not optimal for the present mixed-phase approach because low-density snow particles can melt within only a few thermal-camera frames, providing insufficient temporal resolution for the melting-stage mass calculation. Reducing the plate temperature slows the melting process and increases the number of frames available for estimating the frozen mass. However, reducing the plate temperature also lowers the apparent radiative temperature of the low-emissivity aluminum surface, which can result in a background temperature below 0 °C and reduce the thermal contrast between the plate and melting ice.

Therefore, for mixed-phase measurements, the plate temperature and surface emissivity must be considered together. Increasing the surface emissivity while reducing the plate temperature allows the apparent radiative background temperature to remain approximately 5–10 °C while slowing the melting process. Optimizing this combination can provide sufficient thermal contrast and temporal resolution during both melting and evaporation, enabling the frozen and liquid mass components to be estimated independently.

3. THERMOGRAPHY-BASED PHASE DIFFERENTIATION METHOD

The DEID's thermal camera records each image as a temperature matrix containing both the heated plate and the hydrometeor. The same temperature matrix is processed twice using two different temperature mappings to independently analyze the melting and evaporation stages.

For the melting analysis, the minimum particle temperature in the temperature matrix is assigned to grayscale level 0, while the apparent radiative background temperature is assigned to grayscale level 255. This mapping produces a bright background and dark frozen particles, providing sufficient thermal contrast to determine the particle boundary during melting. The projected frozen-particle area, $A_{ice}(t)$, and the corresponding minimum particle temperature, $T_{ice}(t)$, are then extracted and used in the melting energy balance.

For the evaporation analysis, the same temperature matrix is remapped by assigning 0°C to grayscale level 0 and a temperature slightly above the physical plate temperature to grayscale level 255. With this mapping, temperatures at or below 0 °C appear dark, while the melted liquid portion appears bright against the darker background. The projected liquid area, $A_{liq}(t)$, and the corresponding liquid temperature, $T_{liq}(t)$, are then extracted and used in the evaporation energy balance.

4. LABORATORY VALIDATION & CALIBRATION

Laboratory experiments were conducted in a temperature-controlled cold room maintained at −10°C with an average relative humidity of approximately 15%. The cold-room cooler produced continuous air gusts during the experiments. These conditions promoted sublimation of the small ice particles, introducing an additional source of experimental uncertainty.

Ice particles of different masses were generated using a micropipette with nominal settings corresponding to 1, 2, 4, 6, 8, and 10 mg of water. Individual water droplets were placed between two small plastic weighing trays to produce approximately flat and uniform upper and lower surfaces. Each tray was weighed before use with a balance having a resolution of 0.1 mg, and the actual water mass was determined from the difference between the tray mass before and after addition of the droplet. Because the actual particle masses differed from the nominal micropipette settings, the balance measurements were used as the reference masses throughout the analysis. The prepared particles were frozen at −40°C in a freezer located within the cold room to minimize sublimation prior to testing. After freezing, broken or visibly damaged particles were discarded.

Before each DEID measurement, intact frozen particles were photographed from directly above adjacent to a millimeter scale to provide an independent measurement of projected particle area. Because the DEID infrared camera viewed the hotplate at an angle of approximately 30° from vertical, the particle area obtained from the thermal images was affected by the viewing geometry. The thermal-image particle areas were therefore corrected for the camera viewing angle and evaluated against the independently measured areas obtained from the overhead photographs.

The infrared camera recorded at 30 frames per second. High-emissivity Kapton tape (emissivity ≈ 0.95) was placed around the perimeter of the measurement region to provide a reference for determining the actual hotplate temperature from the thermal images. The hotplate was maintained at approximately 27 °C, which slowed the melting process and provided an adequate number of thermal frames, particularly for the smaller particles. Each frozen particle was placed individually on the hotplate, and its temperature and projected area were recorded continuously through both melting and evaporation. Five particles were tested for each nominal particle mass.

Simultaneous observation of the melting and evaporation processes required careful control of the apparent radiative temperature of the plate, hereafter referred to as the background temperature. A background temperature above 0 °C was required to provide sufficient thermal contrast between the subfreezing ice particle and the aluminum hotplate surface during melting. With the original oxidized aluminum surface, the combination of a 27 °C plate temperature and −10 °C cold-room surroundings resulted in an apparent background temperature of approximately −5.5 to −6.5 °C, providing insufficient contrast for reliable detection of the melting ice. Therefore, the measurement region was coated with a thin layer of black alcohol-based ink, increasing the surface emissivity to approximately 0.75. This modification increased the apparent background temperature to approximately 5−12 °C while maintaining the plate temperature near 27 °C, allowing both the melting and evaporation stages to be resolved.

A separate calibration dataset consisting of ten nominal 5 mg ice particles was initially used to determine a representative $\tilde{k}$ calibration constant for the melting-mass calculation. This value was applied to the remaining particle sizes to evaluate whether a single $\tilde{k}$ could adequately characterize the melting process over the tested mass range.

For image analysis, each thermal frame was converted to grayscale using two temperature mappings corresponding to the melting and evaporation stages. For the melting analysis, temperatures from −12 to 4 °C were mapped to grayscale values from 0 to 255, respectively, providing contrast between the cold ice particle and the warmer background. For the evaporation analysis, temperatures from 0 to 30 °C were mapped to grayscale values from 0 to 255, respectively, isolating the liquid-water region during evaporation. The resulting area and temperature histories were subsequently used in the DEID melting and evaporation energy balances to independently estimate particle mass.

5. FIELD OBSERVATIONS SITES

To demonstrate the proposed methodology under natural precipitation conditions, preliminary field observations were obtained from two sites in northern Utah. The first dataset was collected during the 2019–2020 winter season at a meteorological measurement tower located at the mouth of Red Butte Canyon, Salt Lake City, Utah (40.76857°N, 111.82614°W; elevation 1547 m). The second dataset was collected during the 2025–2026 winter season at the Atwater Snow-Study Plot (40.5912°N, 111.6377°W; elevation 2662 m), a site managed by the Utah Department of Transportation (UDOT), where the University of Utah operates the DEID and additional instrumentation. Red Butte Canyon represents a lower-elevation valley environment, whereas Atwater represents a high-elevation mountain environment where mixed-phase precipitation can occur near the rain–snow transition.

Meteorological observations collected at both sites, together with DEID measurements, were used to evaluate the proposed methodology under natural atmospheric conditions and characterize the temporal occurrence of snow, rain, and mixed-phase precipitation.

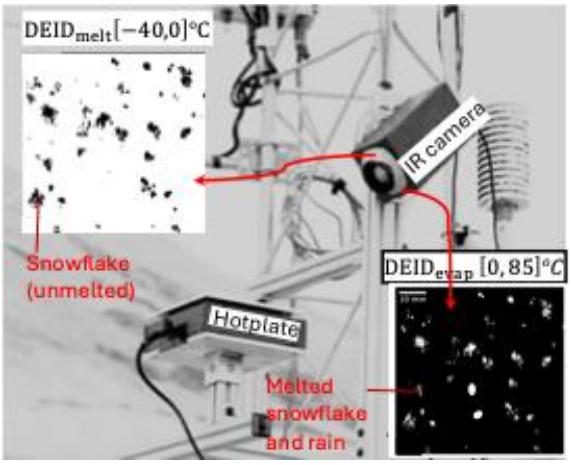


Figure 1. DEID experimental setup deployed at the Red Butte experimental site, showing the hotplate and infrared (IR) camera used for mixed-phase precipitation measurements. Thermal images are processed using two temperature ranges. In the −40 to 0 °C range, unmelted snowflakes appear dark against a bright background. In the 0 to 85 °C range, melted snowflakes and rain appear bright against a dark background, allowing the frozen and liquid hydrometeor components to be distinguished.

6. LABORATORY RESULTS AND DISCUSSION

Accurate determination of particle area is required for the DEID mass calculation. Because the thermal camera viewed the hotplate at approximately 30° from vertical, the detected particle area was corrected for the camera viewing angle and compared with independent measurements obtained from overhead photographs. The close agreement between the two measurements confirmed that the corrected thermal-image area was suitable for the subsequent mass calculations.

Previous DEID studies have shown that a constant $\tilde{k}$ can adequately characterize heat transfer during evaporation (Singh et al., 2021). For the melting experiments, however, application of a single $\tilde{k}$ across the tested particle-mass range produced systematic differences between the DEID-derived melting mass and the reference scale mass, with the largest disagreement observed for the smallest particles. Because the tested particles were small (approximately 1–10 mg), the observed differences may be influenced by experimental uncertainties, including sublimation and small mass losses during handling and transfer to the hotplate. In addition, melting occurred within only a few seconds, increasing the sensitivity of the calculation to particle area, temperature, and timing. Therefore, the observed variation in $\tilde{k}$ cannot presently be attributed solely to a physical dependence on particle size.

To account for this variation, the experimentally determined relationship between maximum particle area and $\tilde{k}$ was used to adjust the melting-mass calculation across the tested particle sizes. Following this adjustment, the DEID-derived melting mass showed strong agreement with the independently measured scale mass (Fig. 2), with a linear-fit slope of approximately 0.99 and $R^2 = 0.97$. This result demonstrates that the melting-stage energy balance can provide an independent estimate of frozen-particle mass over the investigated range.

Currently we have hypothesized that the strong correlation between maximum particle area and the ideal $\tilde{k}$ value for the melting mass is due to the layer of liquid water that surrounds the ice particle as it melts and floats. The correlation between $\tilde{k}$ and particle area was found to be almost perfectly inverse, just as the length scale is inversely related to conductive heat transfer. This may suggest that the liquid creates an insulating effect on the ice that changes the nature of the conductive heating occurring between the plate and the ice.

The independently calculated evaporation mass was then compared with the melting-derived mass (Fig. 3). The two mass estimates were strongly correlated ($R^2 = 0.86$), although the evaporation method showed a small overall overestimation relative to the melting method. The agreement between the independently determined melting and evaporation masses provides preliminary support for using these two thermal processes to separately quantify the frozen and liquid components of mixed-phase hydrometeors.

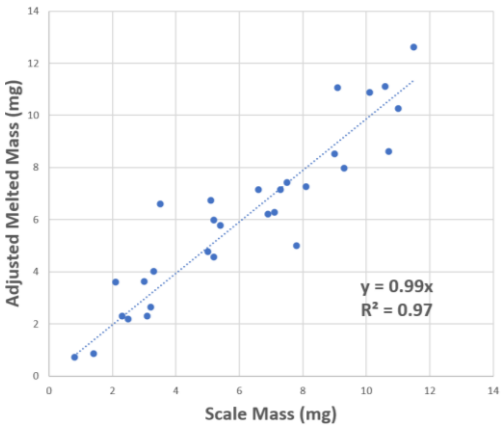


Figure 2. Comparison of reference ice-particle mass measured with the laboratory weighing scale and mass estimated from the DEID melting method after applying the particle-area-dependent $\tilde{k}$ adjustment. The dashed line represents the linear fit.

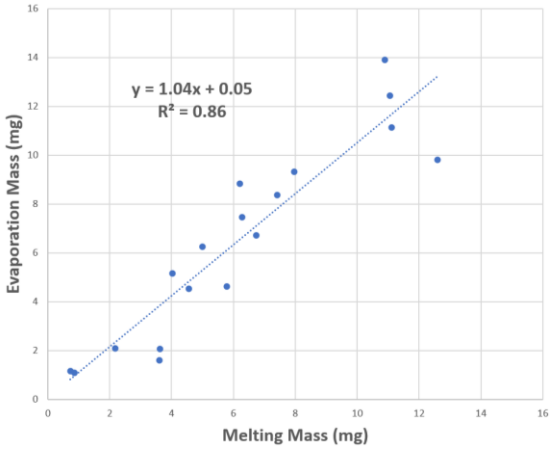


Figure 3. Comparison of particle mass independently estimated from the DEID melting and evaporation methods. The dashed line represents the linear fit.

7. PRELIMINARY FIELD RESULTS

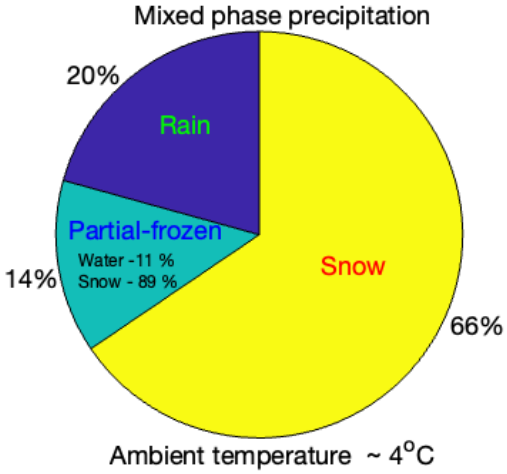


Figure 4. Precipitation-phase measurements obtained using DEID at the Red Butte experimental site on April 18, 2020. Approximately 800 hydrometeors were analyzed at an ambient temperature of approximately 4 °C. The figure shows the classification of the observed hydrometeors into snow, rain, and mixed-phase precipitation, along with the frozen and liquid-water mass fractions of the mixed-phase hydrometeors.

Preliminary field measurements collected at the Red Butte experimental site on April 18, 2020, were used to demonstrate the DEID mixed-phase measurement approach under natural precipitation conditions. Using the melting and evaporation methods, individual hydrometeors were classified as snow, rain, or mixed-phase precipitation, and their frozen and liquid masses were estimated independently. Approximately 66% of the observed hydrometeors were classified as snow, 14% as rain, and 20% as mixed-phase precipitation. For the mixed-phase hydrometeors, the estimated mass partition consisted of approximately 89% frozen mass and 11% liquid water. These preliminary field results demonstrate the potential of DEID to distinguish precipitation phase and quantify the frozen and liquid mass fractions of individual mixed-phase hydrometeors.

8. SUMMARY AND FUTURE WORK

The laboratory experiments demonstrate the feasibility of independently estimating hydrometeor mass using the DEID melting and evaporation methods, providing the basis for particle-by-particle fractionation of mixed-phase precipitation. Future work will focus on further refining the above-described measurement parameters and quantifying measurement uncertainty. Following laboratory optimization, the method will be dEPLOYED AT THE RED BUTTE OR ATWATER FIELD SITE, WHERE ADDITIONAL PRECIPITATION INSTRUMENTATION WILL BE USED TO INDEPENDENTLY VALIDATE THE DEID MIXED-PHASE MEASUREMENTS. THIS FIELD VALIDATION WILL SUPPORT THE DEVELOPMENT OF REAL-TIME MEASUREMENTS OF THE FROZEN AND LIQUID FRACTIONS OF MIXED-PHASE PRECIPITATION.

COMPETEING INTERESTS

The DEID® and Particle Flux Analytics® are registered trademarks. The authors declare the following financial interests and/or personal relationships, which may be considered potential competing interests:

TJG is a scientific advisor for Particle Flux Analytics and holds an equity interest. TJG, DKS, and ERP are named patent holders for the DEID® (No. 11,674,878), which is licensed to Particle Flux Analytics®. ERP and DKS have royalty interest in DEID® sales.

ACKNOWLEDGEMENTS

We thank Steven Clark of the Utah Department of Transportation (UDOT) for his support and direction throughout each winter season. We thank Dave Richards, Johnathan Morgan, and the rest of the Alta Ski Patrol for field support. This material is based upon work partially supported by the National Science Foundation under Grant No. PDM-2210179.

We thank Allan Reaburn and Particle Flux Analytics, Inc. for their contributions to the development and advancement of the DEID. DEID development is also based upon work supported by the U.S. Department of Energy through SBIR Awards

granted to Particle Flux Analytics, Inc. under contract numbers DE-SC0017168, DE-SC0022516, and DE-SC0025812. Particle Flux Analytics Inc. provided technical expertise. Particle Flux Analytics, Inc. owns invention licenses, proprietary data rights, and the copyrights and trademarks for the DEID.

REFERENCES

Fehlmann, M., Rohrer, M., von Lerber, A., and Stoffel, M., 2020. Automated precipitation monitoring with the Thies disdrometer: biases and ways for improvement. *Atmospheric Measurement Techniques* Discussions, 1–31.

Fisher, K. C., Haegeli, P., and Mair, P., 2022. Travel and terrain advice statements in public avalanche bulletins: a quantitative analysis of who uses this information, what makes it useful, and how it can be improved for users, *Nat. Hazards Earth Syst. Sci*., 22, 1973–2000.

García-Benadí, A., Bech, J., González, S., Udina, M., Codina, B., and Georgis, J.-F., 2020. Precipitation Type Classification of Micro Rain Radar Data Using an Improved Doppler Spectral Processing Methodology. *Remote Sensing*, 12, 4113.

Grazioli, J., Tuia, D., Monhart, S., Schneebeli, M., Raupach, T., and Berne, A., 2014. Hydrometeor classification from two-dimensional video disdrometer data. *Atmospheric Measurement Techniques*, 7(9):2869–2882.

Greene, E., Wiesinger, T., Birkeland, K. W., Coleou, C., Jones, A., and Statham, G., 2006. Fatal avalanche accidents and forecasted danger levels: Patterns in the United States, Canada, Switzerland and France, in: Proceedings of the International Snow Science Workshop, Telluride, CO, 1-6 October 2006, 640-649.

Jennings, K. S., Arienzo, M. M., Collins, M., Hatchett, B. J., Nolin, A. W., & Aggett, G., 2023. Crowdsourced data highlight precipitation phase partitioning variability in rain-snow transition zone. *Earth and Space Science*, 10, e2022EA002714.

Jia, X., Liu, Y., Ding, D., Ma, X., Chen, Y., Bi, K., Tian, P., Lu, C., and Quan, J., 2019. Combining disdrometer, microscopic photography, and cloud radar to study distributions of hydrometeor types, size and fall velocity, Atmos. Res., 228, 176–185.

Locatelli, J. D., and Hobbs, P. V., 1974. Fall speeds and masses of solid precipitation particles, J. Geophys. Res., 79(15), 2185–2197.

McClung, D. M. and Schaerer, P. A., 2006. The Avalanche Handbook. 3rd ed, *The Mountaineers*, 347 (pp. 345-359).

Morrison, T. J., Meisenheimer, T., Garrett, T., Singh, D., Donovan, S., and Pardyjak, E., 2023. Relating storm-snow avalanche instabilities to data collected from the Differential Emissivity Imaging Disdrometer (DEID), *Cold Reg. Sci. Technol*., 210, 103839.

Prigent, C., 2010. Precipitation retrieval from space: An overview, *C. R. Geosci*., 342, 380–389.

Singh, D. K., Donovan, S., Pardyjak, E. R., and Garrett, T. J., 2021. A differential emissivity imaging technique for measuring hydrometeor mass and type, *Atmos. Meas. Tech.*, 14, 6973–6990.

Singh, D.K., Pardyjak, E. R., and Garrett, T. J., 2023. A universal scaling law for Lagrangian snowflake accelerations in atmospheric turbulence. *Physics of Fluids*, 35(12), 123336.

Singh, D. K., Pardyjak, E. R., and Garrett, T. J., 2024. Time-resolved measurements of the densities of individual frozen hydrometeors and fresh snowfall, *Atmos. Meas. Tech*., 17, 4581–4598.

Zhao, R., Wang, K., & Xu, X., 2024. A machine learning method to retrieve global rainfall and snowfall rates from the passive microwave observations of FY-3E. *Journal of Geophysical Research: Atmospheres*, 129, e2024JD040731.